Effect of material inhomogeneity on the rotating functionally of a graded orthotropic hollow cylinder [†]

H. M. Wang[*]

Department of Mechanics, Zhejiang University, Hangzhou 310027, P. R. China

---

Abstract

The effect of the material inhomogeneity on the stress field of a rotating orthotropic infinite hollow cylinder made of functionally graded materials is investigated. The original functionally graded hollow cylinder is approximated by the laminate model, of which the solution will gradually approach the exact one with the increase in number of fictitious layers. The analysis is performed by means of the state space method. The validity of the solution is verified by utilizing the exact solution of a special non-homogeneous rotating hollow cylinder and earlier results. The distributions of the radial and tangential stresses of the internally pressurized rotating functionally graded hollow cylinder for various material inhomogeneity parameters are depicted graphically. The degree of the orthotropy on the stress fields is also discussed.

Keywords: Functionally graded material; Rotating hollow cylinder; Elastic analysis; State space method; Laminate model

---

1. Introduction

Rotating disks and cylinders have important applications in rotating machinery and structures, such as flywheels, steam and gas turbines, high-speed cameras, planetary landings, etc. The stress analysis of rotating homogeneous isotropic, orthotropic, and anisotropic disks and cylinders has long been an important topic in engineering design and applications [1-6].

The concept of functionally graded materials can be considered in order to make optimal use of the material. The material properties of the FGM vary continuously and the stress distribution can be adjusted ideally. Many investigations for rotating FGM disks and cylinders exist in the literature. Reddy and Srinath [7] studied the elastic stresses in a rotating anisotropic annular disk of variable density. Horgan and Chan [8] dealt with the stress response of functionally graded isotropic linearly elastic rotating disks. El-Naggar et al. [9] handled the thermal stresses in a rotating non-homogeneous orthotropic hollow cylinder. Eraslan and Akis [10] obtained the plane strain and plane stress solutions of a functionally graded rotating solid shaft and solid disk. Zenkour [11] investigated stress distribution in rotating composite structures of functionally graded solid disks. Chen et al. [12] obtained the three-

dimensional analytical solution of rotating functionally graded disks.

For a special non-homogeneous material with material properties that have power law dependence with radial distance, the analytical solution for rotating disks and cylinders can be cited in Refs. [7, 8, 10]. For rotating hollow disks and cylinders made of functionally graded materials with general form, obtaining the exact solution is very difficult or impossible. The objective of this work is to develop an effective way to analyze the distribution of the stresses in a rotating functionally graded orthotropic hollow cylinder with a general variation in form of its material properties by using the laminate model.

2. Problem statements

Consider a long hollow cylinder with interior radius a and exterior radius b rotating at a constant angular velocity ω about its central axis. The case under consideration can be treated as an axisymmetric plane strain problem. In the cylindrical coordinate system (r, θ, z), $u_r(r)$ is the only non-zero component of the displacement and is only the function of radial coordinate r. Suppose both the elastic constants c_{jk} ($j, k = 1, 2$) and the mass density ρ of the functionally graded materials are functions of radial position—that is

$$c_{jk} = c_{jk}(r), \quad \rho = \rho(r) \tag{1}$$

If the material properties are characterized as cylindrically

orthotropic, the constitutive relations are

$$\sigma_{rr} = c_{11}\frac{du_r}{dr} + c_{12}\frac{u_r}{r}, \quad \sigma_{\theta\theta} = c_{12}\frac{du_r}{dr} + c_{22}\frac{u_r}{r} \tag{2}$$

where σ_{rr} and $\sigma_{\theta\theta}$ are radial and tangential stresses, respectively. The equation of equilibrium is

$$\frac{d\sigma_{rr}}{dr} + \frac{\sigma_{rr} - \sigma_{\theta\theta}}{r} + \rho\omega^2 r = 0 \tag{3}$$

Suppose the hollow cylinder is subjected to uniform pressures Q_a and Q_b at the interior and exterior surfaces, respectively. The boundary conditions are expressed as

$$\sigma_{rr}(a) = Q_a, \quad \sigma_{rr}(b) = Q_b \tag{4}$$

3. Analytical model and mathematical development

The laminate approximation method is an effective way to analyze the FGM problem. Physically, the solution of the laminated model will gradually approach the exact one with an increase in the number of fictitious layers. Suppose the functionally graded hollow cylinder is divided into n sublayers. From the inner to outer layers, the discrete radius is denoted as $r_i (i = 0, 1, \cdots, n)$. Particularly, we have $r_0 = a$ and $r_n = b$. For each sub-layer $r_{i-1} \le r \le r_i$ $(i = 1, 2, \cdots, n)$, the material properties are treated as constants. In this study, the material constants for each layer are treated as

$$c_{jk}^{(i)} = c_{jk}(r_i), \quad \rho^{(i)} = \rho(r_i) \quad (i = 1, 2, \cdots, n) \tag{5}$$

For the sake of convenience, the following non-dimensional quantities and variables are introduced as

$$\overline{c}_{jk}^{(i)} = \frac{c_{jk}^{(i)}}{c_{11}^{(n)}}, \quad \overline{\rho}^{(i)} = \frac{\rho^{(i)}}{\rho^{(n)}}, \quad u^{(i)} = \frac{u_r^{(i)}}{b}, \quad \sigma_r^{(i)} = \frac{\sigma_{rr}^{(i)}}{c_{11}^{(n)}}, \quad \sigma_\theta^{(i)} = \frac{\sigma_{\theta\theta}^{(i)}}{c_{11}^{(n)}},$$
$$\xi = \frac{r}{b}, \quad \xi_i = \frac{r_i}{b}, \quad \Omega = \frac{\omega}{c_v}b, \quad c_v = \sqrt{\frac{c_{11}^{(n)}}{\rho^{(n)}}}, \quad q_a = \frac{Q_a}{c_{11}^{(n)}}, \quad q_b = \frac{Q_b}{c_{11}^{(n)}} \tag{6}$$

Then for the discrete system, the governing equations (2)-(4) can be rewritten as

$$\sigma_r^{(i)} = \overline{c}_{11}^{(i)}\frac{du^{(i)}}{d\xi} + \overline{c}_{12}^{(i)}\frac{u^{(i)}}{\xi}, \quad \sigma_\theta^{(i)} = \overline{c}_{12}^{(i)}\frac{du^{(i)}}{d\xi} + \overline{c}_{22}^{(i)}\frac{u^{(i)}}{\xi}$$
$$(i = 1, 2, \cdots, n) \tag{7}$$

$$\frac{d\sigma_r^{(i)}}{d\xi} + \frac{\sigma_r^{(i)} - \sigma_\theta^{(i)}}{\xi} + \overline{\rho}^{(i)}\Omega^2\xi = 0 \quad (i = 1, 2, \cdots, n) \tag{8}$$

$$\sigma_r^{(1)}(\xi_0) = q_a, \quad \sigma_r^{(n)}(\xi_n) = q_b \tag{9}$$

At each fictitious interface in the laminate model, the continuity conditions should be completed as

$$u^{(i)}(\xi_i) = u^{(i+1)}(\xi_i), \quad \sigma_r^{(i)}(\xi_i) = \sigma_r^{(i+1)}(\xi_i) \ (i = 1, 2, \cdots, n-1) \tag{10}$$

4. Solution for laminate model

Eqs. (7)-(10) can be rewritten as

$$\Sigma_r^{(i)} = \overline{c}_{11}^{(i)}\nabla u^{(i)} + \overline{c}_{12}^{(i)}u^{(i)}, \quad \Sigma_\theta^{(i)} = \overline{c}_{12}^{(i)}\nabla u^{(i)} + \overline{c}_{22}^{(i)}u^{(i)}$$
$$(i = 1, 2, \cdots, n) \tag{11}$$

$$\nabla\Sigma_r^{(i)} - \Sigma_\theta^{(i)} + \overline{\rho}^{(i)}\Omega^2\xi^3 = 0 \quad (i = 1, 2, \cdots, n) \tag{12}$$

$$\Sigma_r^{(1)}(\xi_0) = \xi_0 q_a, \quad \Sigma_r^{(n)}(\xi_n) = \xi_n q_b \tag{13}$$

$$u^{(i)}(\xi_i) = u^{(i+1)}(\xi_i), \quad \Sigma_r^{(i)}(\xi_i) = \Sigma_r^{(i+1)}(\xi_i) \quad (i = 1, 2, \cdots, n-1) \tag{14}$$

where

$$\Sigma_r^{(i)} = \xi\sigma_r^{(i)}, \quad \Sigma_\theta^{(i)} = \xi\sigma_\theta^{(i)}, \quad \nabla = \xi\frac{d}{d\xi} \tag{15}$$

We first obtain the expression for $\nabla u^{(i)}$ from the first part of Eq. (11), then substitute $\Sigma_\theta^{(i)}$ in the second part of Eq. (11) into Eq. (12). Having obtained the expression for $\nabla u^{(i)}$, the expression for $\nabla\Sigma_r^{(i)}$ is derived. The expressions of $\nabla u^{(i)}$ and $\nabla\Sigma_r^{(i)}$ can be recast in matrix form as

$$\nabla\{X^{(i)}\} = [N^{(i)}]\{X^{(i)}\} + \{L^{(i)}\}\xi^3 \tag{16}$$

where

$$\{X^{(i)}\} = \begin{Bmatrix} u^{(i)} \\ \Sigma_r^{(i)} \end{Bmatrix}, \quad [N^{(i)}] = \begin{bmatrix} a_{11}^{(i)} & a_{12}^{(i)} \\ a_{21}^{(i)} & a_{22}^{(i)} \end{bmatrix}, \quad \{L^{(i)}\} = \begin{Bmatrix} 0 \\ -\overline{\rho}^{(i)}\Omega^2 \end{Bmatrix}$$
$$a_{11}^{(i)} = -\frac{\overline{c}_{12}^{(i)}}{\overline{c}_{11}^{(i)}}, \quad a_{12}^{(i)} = \frac{1}{\overline{c}_{11}^{(i)}}, \quad a_{21}^{(i)} = \overline{c}_{22}^{(i)} + \overline{c}_{12}^{(i)}a_{11}^{(i)}, \quad a_{22}^{(i)} = \overline{c}_{12}^{(i)}a_{12}^{(i)} \tag{17}$$

The solution of Eq. (16) is

$$\{X^{(i)}(\xi)\} = [T^{(i)}(\xi)]\big(\{X^{(i)}(\xi_{i-1})\} + \{G^{(i)}(\xi)\}\big) \quad (i = 1, 2, \cdots, n) \tag{18}$$

where

$$[T^{(i)}(\xi)] = \left(\frac{\xi}{\xi_{i-1}}\right)^{[N^{(i)}]}, \quad \{G^{(i)}(\xi)\} = \int_{\xi_{i-1}}^{\xi}[T^{(i)}(\eta)]^{-1}\{L^{(i)}\}\eta^2 d\eta \tag{19}$$

The continuity conditions (10) can be rewritten as

$$\{X^{(i)}(\xi_i)\} = \{X^{(i+1)}(\xi_i)\} \ (i = 1, 2, \cdots, n-1) \tag{20}$$

Setting $\xi = \xi_i$ in Eq. (18) and utilizing Eq. (20), we have

$$\{X^{(i)}(\xi_i)\} = [H^{(i)}]\{X^{(1)}(\xi_0)\} + \{M^{(i)}\} \tag{21}$$

where

$$[H^{(i)}] = [\tilde{T}_1^{(i)}],$$
$$\{M^{(i)}\} = \sum_{m=1}^{i}[\tilde{T}_m^{(i)}]\{G^{(m)}(\xi_m)\}, \quad [\tilde{T}_m^{(i)}] = \prod_{j=i}^{m}[T^{(j)}(\xi_j)] \tag{22}$$

If $i = n$, by means of the boundary conditions (13), Eq. (21) can be rewritten as

$$\begin{Bmatrix} u^{(n)}(\xi_n) \\ \xi_n q_b \end{Bmatrix} = \begin{bmatrix} H_{11}^{(n)} & H_{12}^{(n)} \\ H_{21}^{(n)} & H_{22}^{(n)} \end{bmatrix} \begin{Bmatrix} u^{(1)}(\xi_0) \\ \xi_0 q_a \end{Bmatrix} + \begin{Bmatrix} M_1^{(n)} \\ M_2^{(n)} \end{Bmatrix} \tag{23}$$

Then $u^{(1)}(\xi_0)$ can be determined from the second part of Eq. (23) as

$$u^{(1)}(\xi_0) = \frac{1}{H_{21}^{(n)}}(\xi_n q_b - H_{22}^{(n)}\xi_0 q_a - M_2^{(n)}) \tag{24}$$

Utilizing Eqs. (20) and (21), Eq. (18) can be written in a detailed form as

$$\begin{Bmatrix} u^{(i)}(\xi) \\ \Sigma_r^{(i)}(\xi) \end{Bmatrix} = \begin{bmatrix} T_{11}^{(i)}(\xi) & T_{12}^{(i)}(\xi) \\ T_{21}^{(i)}(\xi) & T_{22}^{(i)}(\xi) \end{bmatrix}$$
$$\left(\begin{bmatrix} H_{11}^{(i-1)} & H_{12}^{(i-1)} \\ H_{21}^{(i-1)} & H_{22}^{(i-1)} \end{bmatrix} \begin{Bmatrix} u^{(1)}(\xi_0) \\ \xi_0 q_a \end{Bmatrix} + \begin{Bmatrix} M_1^{(i-1)} \\ M_2^{(i-1)} \end{Bmatrix} + \begin{Bmatrix} G_1^{(i)}(\xi) \\ G_2^{(i)}(\xi) \end{Bmatrix} \right) \tag{25}$$

Substituting Eq. (24) into Eq. (25), $u^{(i)}(\xi)$ is then completely determined as

$$u^{(i)}(\xi) = f_1^{(i)}(\xi)q_b + f_2^{(i)}(\xi)q_a + f_3^{(i)}(\xi) \tag{26}$$

where

$$f_1^{(i)}(\xi) = \xi_n \left(\frac{H_{11}^{(i-1)}}{H_{21}^{(n)}} T_{11}^{(i)}(\xi) + \frac{H_{21}^{(i-1)}}{H_{21}^{(n)}} T_{12}^{(i)}(\xi) \right)$$
$$f_2^{(i)}(\xi) = \xi_0 \left[\left(H_{12}^{(i-1)} - \frac{H_{22}^{(n)}}{H_{21}^{(n)}} H_{11}^{(i-1)} \right) T_{11}^{(i)}(\xi) \right.$$
$$\left. + \left(H_{22}^{(i-1)} - \frac{H_{22}^{(n)}}{H_{21}^{(n)}} H_{21}^{(i-1)} \right) T_{12}^{(i)}(\xi) \right] \tag{27}$$
$$f_3^{(i)}(\xi) = \left(M_1^{(i-1)} - \frac{M_2^{(n)}}{H_{21}^{(n)}} H_{11}^{(i-1)} + G_1^{(i)}(\xi) \right) T_{11}^{(i)}(\xi)$$
$$+ \left(M_2^{(i-1)} - \frac{M_2^{(n)}}{H_{21}^{(n)}} H_{21}^{(i-1)} + G_2^{(i)}(\xi) \right) T_{12}^{(i)}(\xi)$$

Substituting Eq. (26) into Eq. (7), the stress fields are then determined.

5. Exact solution for power-law graded form

The exact solution for a special functionally graded rotating hollow cylinder will be developed in this section. The material properties are assumed to vary as power-law dependence of the radial position

$$c_{jk}(r) = r^{2\alpha}c_{0jk}, \quad \rho(r) = r^{2\beta}\rho_0 \tag{28}$$

where c_{0jk} and ρ_0 are constants. α and β, denoting the degree of the material inhomogeneity, can be arbitrary rational constants. Replacing $c_{11}^{(n)}$ by c_{011} and $\rho^{(n)}$ by ρ_0 in Eq. (6), the non-dimensional variables and quantities are still adoptable and the general closed-form solution can be obtained as

$$u(\xi) = A_1 \xi^{p_1} + A_2 \xi^{p_2} + B\xi^{2(\beta-\alpha)+3} \tag{29}$$

where

Table 1. Results for $a/b = 0.5$, $\alpha = 0.5$ and $\beta = 0.5$.

n	$u(\xi_0)$	$u(\xi_n)$	$\sigma_r(\xi_{n/2})$	$\sigma_\theta(\xi_0)$	$\sigma_\theta(\xi_n)$
20	0.19876	0.26308	0.060552	0.42691	0.53817
50	0.19898	0.26333	0.059934	0.41519	0.53868
200	0.19908	0.26344	0.059624	0.40929	0.53891
500	0.19910	0.26347	0.059561	0.40811	0.53896
Exact solution	0.19911	0.26348	0.059520	0.40732	0.53899

Table 2. Results for $a/b = 0.5$, $\alpha = 1.0$ and $\beta = 0.5$.

n	$u(\xi_0)$	$u(\xi_n)$	$\sigma_r(\xi_{n/2})$	$\sigma_\theta(\xi_0)$	$\sigma_\theta(\xi_n)$
20	0.26147	0.33168	0.037086	0.29485	0.67850
50	0.26431	0.33505	0.036476	0.28126	0.68539
200	0.26573	0.33674	0.036169	0.27452	0.68886
500	0.26601	0.33709	0.036108	0.27317	0.68956
Exact solution	0.26620	0.33731	0.036067	0.27227	0.69002

Table 3. Results for $a/b = 0.2$, $\alpha = -1.0$ and $\beta = -0.5$.

n	$u(\xi_0)$	$u(\xi_n)$	$\sigma_r(\xi_{n/2})$	$\sigma_\theta(\xi_0)$	$\sigma_\theta(\xi_n)$
20	0.013786	0.099091	0.33467	2.44807	0.20271
50	0.012981	0.096550	0.34238	2.84586	0.19751
200	0.012608	0.095300	0.34637	3.09868	0.19495
500	0.012535	0.095051	0.34718	3.15470	0.19444
Exact solution	0.012488	0.094886	0.34772	3.19317	0.19410

$$p_1 = -\alpha + \sqrt{\alpha^2 + H}, \quad p_2 = -\alpha - \sqrt{\alpha^2 + H}$$
$$B = \frac{\Omega^2}{c_{022} - 2\alpha c_{012} - c_{011}(2\beta + 3)[2(\beta - \alpha) + 3]},$$
$$H = \frac{c_{022} - 2\alpha c_{012}}{c_{011}} \tag{30}$$

In Eq. (29), A_1 and A_2 are unknown constants. Substituting Eq. (29) into Eq. (7), the expressions for radial and tangential stresses can be derived. A_1 and A_2 can be determined completely by utilizing the boundary conditions (13). Specifically, if we set $\alpha=\beta$ in Eq. (28), the present solution is then degenerated to that considered by El-Naggar et al. [13].

6. Numerical results

The validity of the presented solution in Section 5 will first be considered. In the following, the exact solution Eq. (29) will be introduced to examine the validity of the present solution. For the sake of using the present solution Eq. (26), the interval $[\xi_0, \xi_n](\xi_n = 1)$ is fictitiously divided into n equal sub-intervals. In the numerical computations, we take $\bar{c}_{11} = 1.0000$, $\bar{c}_{12} = -0.2308$, $\bar{c}_{22} = 2.0989$, $\Omega = 1$, $q_a = 0$, $q_b = 0$. The displacement, radial and tangential stresses for different values of $\xi_0 = a/b$, α, β and n are listed in Tables 1-3.
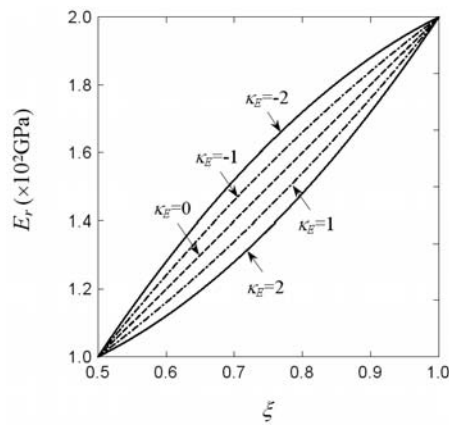
Tables 1-3 show the results obtained by means of the pre-

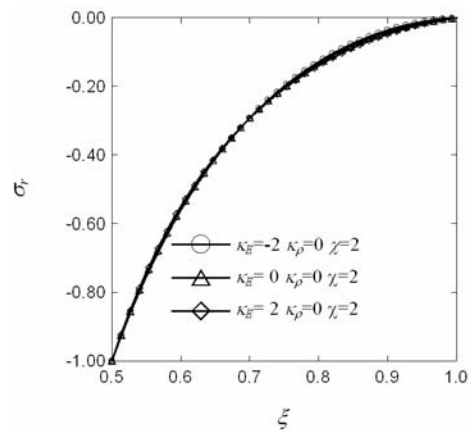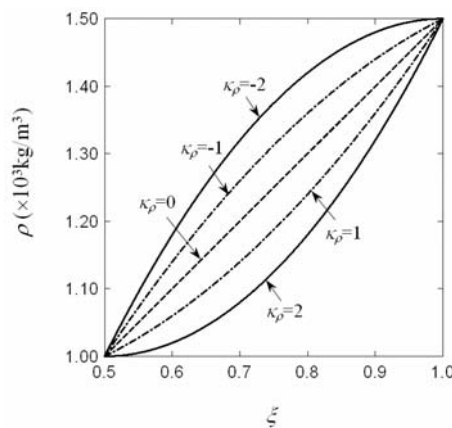Fig. 1. Variation of radial direction Young's modulus $E_r(\xi)$.

Fig. 2. Variation of mass density $\rho(\xi)$.

Fig. 3. Distributions of radial stress for different values of κ_E.

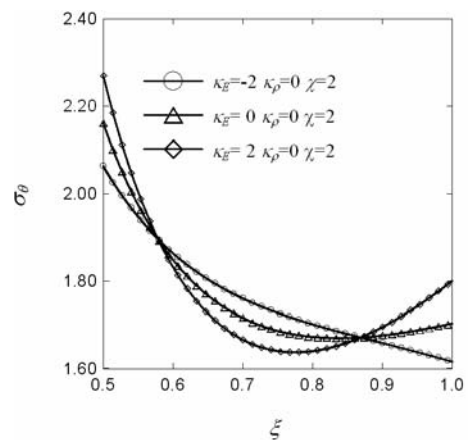

Fig. 4. Distributions of tangential stress for different values of κ_E.

sent solution when different values of $\xi_0 = a/b$, α and β are employed. We found that with an increasing number of fictitious layers, n, the results approach the exact solution gradually. Numerical tests also denote that the present solution is effective in analyzing the distributions of the displacement and stresses in a rotating functionally graded hollow cylinder.

It is noted here that the linearly graded hollow cylinder has been investigated by Shi et al. [14]. By employing the developed method in this investigation and utilizing a laminate model with 1000 fictitious sub-interval layers to approximate the linearly graded hollow cylinder, the obtained results were found to agree well with those presented in Ref. [14]. The correctness of the present method is further clarified.

In the following, the analysis of functionally graded hollow cylinders with general form will further be investigated. Furthermore, the effect of the inhomogeneity and orthotropy will be discussed. Suppose the Young's moduli in radial direction of the hollow cylinder at the interior and exterior surfaces are taken as E_{0r} =100GPa (interior) and E_{1r} =200GPa (exterior). The densities of the hollow cylinder at the interior and exterior surfaces are assumed as ρ_0 =1.0×10³kg/m³ and ρ_1 =1.5×10³ kg/m³, respectively. The variation forms of Young's modulus and the density obey

$$E_r(\xi) = \frac{\xi_n - \xi}{\xi_n - \xi_0} E_{0r} + \frac{\xi - \xi_0}{\xi_n - \xi_0} E_{1r} + \kappa_E E_{0r}(\xi - \xi_0)(\xi - \xi_n)$$

$$\rho(\xi) = \frac{\xi_n - \xi}{\xi_n - \xi_0} \rho_0 + \frac{\xi - \xi_0}{\xi_n - \xi_0} \rho_1 + \kappa_\rho \rho_0(\xi - \xi_0)(\xi - \xi_n) \quad (31)$$

where κ_E and κ_ρ are constants denoting the degree of the inhomogeneity. In the numerical studies, we employ

$$E_\theta(\xi) = E_z(\xi) = \chi E_r(\xi), \quad \upsilon_{\theta r} = \upsilon_{zr} = \upsilon_{z\theta} = 0.3 \quad (32)$$

where χ is also a constant, denoting the degree of the orthotropy. $E_\theta(\xi)$ and $E_z(\xi)$ are Young's moduli in tangential and axial directions, and $\upsilon_{\theta r}$, υ_{zr} and $\upsilon_{z\theta}$ are Poisson's ratios. The elastic constant c_{jm} can be obtained on the basis of the presented Young's moduli and Poisson's ratios [15]. The other calculation parameters are adopted here as $a/b = 0.5$, $\Omega = 1$, $q_a = -1$ and $q_b = 0$. In order to obtain the result with high accuracy, 1000 fictitious sub-interval layers (with equal thickness) are employed in the following computation.

The variation form of the Young's moduli and the density for different values of κ_E and κ_ρ are illustrated graphically
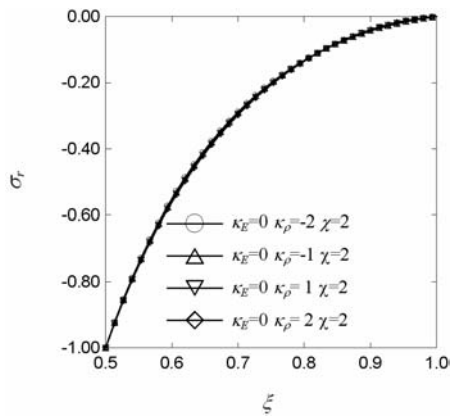
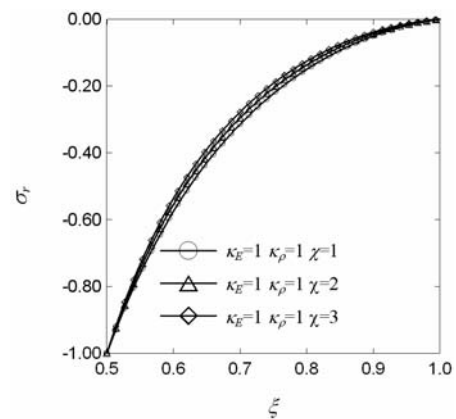Fig. 5. Distributions of radial stress for different values of κ_ρ.

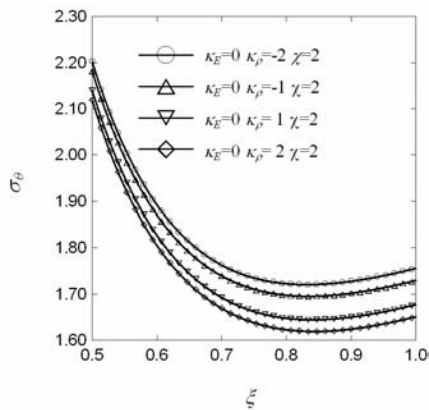Fig. 7. Distributions of radial stress for different values of χ.

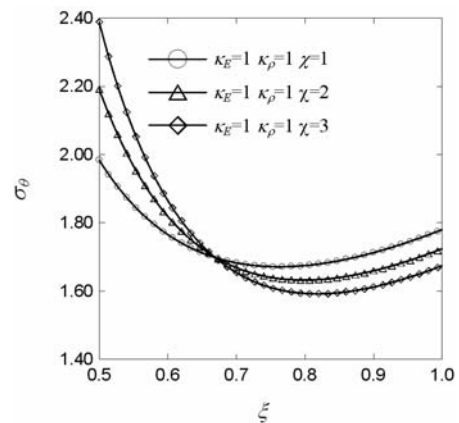Fig. 6. Distributions of tangential stress for different values of κ_ρ.

Fig. 8. Distributions of tangential stress for different values of χ.

in Figs. 1 and 2. It is noted that the cases for $\kappa_E =0$ and $\kappa_\rho =0$ denote that the Young's moduli and the density of the functionally graded hollow cylinder vary linearly with the dependence on the radial coordinate in the hollow cylinder.

The distributions of radial and tangential stresses in an inner pressurized functionally graded hollow cylinder for different values of κ_E (κ_ρ=0, χ=2) are depicted in Figs. 3 and 4, respectively. We find that the inhomogeneity factor of Young's modulus κ_E has little effect on the distributions of radial stress, while the distributions of tangential stress are sensitive to κ_E. At both the interior and exterior surfaces, the tangential stresses increase with the increasing of κ_E. In the middle zone, it does the opposite. To interpret this phenomenon, we recall Fig. 1. It can be seen that the Young's modulus of the functionally graded hollow cylinder at the middle zone decreases with increasing κ_E while those at the internal and external surfaces keep constant. The decrease of the Young's modulus at the middle zone leads to the redistribution of the tangential stress in the functionally graded hollow cylinder. As a result, the part with a low Young's modulus undertakes low tangential stress and hence increases the tangential stress at other parts of the cylinder.

Figs. 5 and 6 show the effect of the inhomogeneity factor of mass density κ_ρ (κ_E=0, χ=2) on the distributions of radial and tangential stresses. Interestingly, κ_ρ has little effect on

the distributions of radial stress while the tangential stresses in a whole cross section decrease with the increasing of κ_ρ. This is physically reasonable. From Fig. 2, we notice that the density of the functionally graded hollow cylinder at the middle zone decreases with the increase of κ_ρ. In fact, the increase of κ_ρ finally leads to the decrease of the inertial force and hence causes the decrease of the tangential tensile stress.

The effect of the degree of material orthotropy χ (κ_E=1, κ_ρ=1) on the distributions of the radial and tangential stresses are illustrated in Figs. 7 and 8. Fig. 7 denotes that the radial stresses have little dependence on χ. While χ plays an important role on the distributions of the tangential stresses, see Fig. 8. We also notice that the distribution of tangential stress in an inner pressurized rotating functionally graded hollow cylinder for χ=1 is more homogeneous than those for χ=2 and χ=3.

7. Conclusions

The pressurized rotating functionally graded hollow cylinder is analyzed by the laminate model. By means of the state space method, the analytical solution for the laminate model is developed in explicit form. The analysis scheme involves only the operations of 2×2 matrices, regardless of the number of fictitious layers. Numerical calculation can be easily per-

formed.

Numerical results denote that the material inhomogeneity and the degree of orthotropy have minor effects on the distributions of radial stress, while having significant effect on the distributions of tangential stress. For engineering applications, the present solution can be employed in selecting the proper material parameters for the pressurized functionally graded rotating hollow cylinder.

Acknowledgments

References

[1] S. P. Timoshenko and J. N. Goodier, *Theory of Elasticity, third ed.,* McGraw-Hill, New York, USA (1970).

[2] C. I. Chang, The anisotropic rotating disks, *Int. J. Mech. Sci.,* 17 (5) (1975) 397-402.

[3] G. Genta and M. Gola, The stress distribution in orthotropic rotating disks, *ASME J. Appl. Mech.,* 48 (3) (1981) 559-562.

[4] N. Tutuncu, Effect of anisotropy on stresses in rotating discs, *Int. J. Mech. Sci.,* 37 (8) (1995) 873-881.

[5] F. Zhou and A. Ogawa, Elastic solutions for a solid rotation disk with cubic anisotropy, *ASME J. Appl. Mech.,* 69 (1) (2002) 81-83.

[6] A. M. Zenkour, Rotating variable-thickness orthotropic cylinder containing a solid core of uniform-thickness, *Arch. Appl. Mech.,* 76 (1-2) (2006) 89-102.

[7] T. Y. Reddy and H. Srinath, Elastic stresses in a rotating anisotropic annular disk of variable thickness and variable density, *Int. J. Mech. Sci.,* 16 (2) (1974) 85-89.

[8] C. O. Horgan and A. M. Chan, The stress response of functionally graded isotropic linearly elastic rotating disks, *J. Elast.,* 55 (3) (1999) 219-230.

[9] A. M. El-Naggar, A. M. Abd-Alla, M. A. Fahmy and S. M. Ahmed, Thermal stresses in a rotating non-homogeneous orthotropic hollow cylinder, *Heat Mass Transfer,* 39 (1) (2002) 41-46.

[10] A. N. Eraslan and T. Akis, On the plane strain and plane stress solutions of functionally graded rotating solid shaft and solid disk problems, *Acta Mech.,* 181 (1-2) (2006) 43-63.

[11] A. M. Zenkour, Stress distribution in rotating composite structures of functionally graded solid disks, *J. Mater. Process. Tech.,* 209 (7) (2009) 3511-3517.

[12] J. Y. Chen, H. J. Ding and W.Q. Chen, Three-dimensional analytical solution for a rotating disc of functionally graded materials with transverse isotropy, *Arch. Appl. Mech.,* 77 (4) (2007) 241-251.

[13] A. M. El-Naggar, A. M. Abd-Alla and S. M. Ahmed, On the rotation of a non-homogeneous composite infinite cylinder of orthotropic material, *Appl. Math. Comput.,* 69 (2-3) (1995) 147-157.

[14] Z. F. Shi, T. T. Zhang and H.J. Xiang, Exact solution of heterogeneous elastic hollow cylinders, *Compos. Struct.,* 79 (1) (2007) 140-147.

[15] S. G. Lekhnitskii, *Theory of elasticity of an anisotropic body*, Mir Publishers, Moscow, Russia, (1981).

Huiming Wang received the B.S. and M.S. degrees in engineering mechanics from Dalian University of Technology, Dalian, China in 1994 and 1997 respectively and the Ph.D. degree in solid mechanics from Zhejiang University, Hangzhou, China in 2003. He is currently an associate professor at the Department of Engineering Mechanics, Zhejiang University. His research focuses on elastic analysis and control of piezoelectric structures and systems.